SASEC2015
Third Southern African Solar Energy Conference
11–13 May 2015
Kruger National Park, South Africa

NEW CONCEPT OF SOLAR THERMAL POWER GENERATION COMBINED WITH ALUMINUM AND SUPERCRITICAL CO2 GAS TURBINE

Muto Y.,* Kato Y., Aritomi M., Ishizuka T. and Watanabe N.
*Author for correspondence
Research Laboratory for Nuclear Reactors
Tokyo Institute of Technology
2-12-1, O-okayama, Meguro-ku, Tokyo, 152-8550
Japan
E-mail: muto@nr.titech.ac.jp

ABSTRACT

Existing tower type solar power plants consist of a sunbeam collecting system of a solar power tower with heliostats, a molten salt heat transfer and heat storage system, and a steam turbine power generation system. In a new system, the molten salt is replaced by aluminum. The steam turbine is replaced by a supercritical CO_2 gas turbine, which can achieve 48% cycle thermal efficiency with turbine inlet temperature of 650°C. In addition, the concentrating power tower is replaced by a beam-down solar system to reduce the radiation loss at the receiver. The aluminum receiver structure and dimensions are shown based on the simplified heat transfer analyses. For the 100 MWt receiver inlet energy, the available power becomes 40.1 MWe at daytime and 8.1 MWe at night.

INTRODUCTION

Although the solar energy is sustainable and desirable, with no environmentally detrimental effects, the present power generation cost is extremely high. The cost is considerably higher even than for renewable energy of other types such as wind power. Therefore, solar power cost reduction is earnestly sought. As described in this paper, the tower type solar thermal power generation is considered among other solar power systems such as photovoltaic, trough, and dish. Improvement of the cycle thermal efficiency is effective to achieve cost reduction. Because the cycle thermal efficiency of the steam turbine is limited to around 40%, replacement by a gas turbine is desirable to achieve higher efficiency by increasing the turbine inlet temperature. However, for the molten salt, the highest available temperature is less than 600°C. Therefore, the use of aluminum is considered instead of the molten salt. The aluminum is useful at higher temperatures. It is an extremely good heat transfer material with high thermal conductivity of 230 W/m/K. Additionally, it melts at 660°C and its heat of fusion is extremely large, i.e., 0.397 MJ/kg. Therefore, aluminum can receive the collected solar heat with a small temperature difference. The heat is stored and transferred to the working gas effectively because the working gas, supercritical CO_2 is appropriate for the task. The critical condition of CO_2 is 7.38 MPa and 31.06°C. When CO_2 is compressed to a supercritical condition, the compression work becomes slight compared with ideal gas compression. Then, the cycle thermal efficiency of the supercritical CO_2 cycle becomes considerably higher than an ideal gas turbine cycle such as a helium turbine cycle [1, 2, 3]. When the receiver surface temperature is raised, a radiation heat loss increases markedly, which is proportional to the fourth power of the absolute temperature. For this problem, a beam down system [4] becomes a good solution. In the beam down system, the receiver has a bottle shape. Sun beams are introduced from the upper inlet to the bottle shape receiver. Although the inside wall of the receiver becomes high and although many radiation beams are emitted, most of these are stored with the bottle because leakage is only possible through the upper bottleneck opening.

The structure of the beam down receiver surrounded by the aluminum blanket is described next. Simplified one-dimensional heat transfer analyses are conducted for the aluminum receiver. The cycle performance of the supercritical CO_2 gas turbine is shown with an energy flow diagram.

NOMENCLATURE

η_{total}	[-]	Total thermal efficiency
$\eta_{receiver}$	[-]	Ratio of the transferred energy to working fluid versus the solar beam energy collected at the receiver surface
η_{cycle}	[-]	Power generation efficiency of the turbine cycle
N_{row}	[-]	Number of tube row
$N_{tube,m}$	[-]	Number of tubes within a module
N_m	[-]	Number of modules
$N_{tube,av,row}$	[-]	Number of tubes in a fan-shaped area
D_{out}	[m]	Outer diameter of heat transfer tube
D_{in}	[m]	Inner diameter of heat transfer tube
D_2	[m]	Outer diameter of receiver vessel
D_1	[m]	Inner diameter of receiver vessel
ts	[m]	Module shell thickness
L_m	[m]	Module radial length
L_{eff}	[m]	Effective length of module
Pitch	[m]	Pitch for the tube arrangement
$L_{heat\ transfer}$	[m]	Effective heat transfer length
$S_{eff,m}$	[m2]	Effective area in a module
S_{unit}	[m2]	Unit area for the tube arrangement
$S_{Al,m}$	[m2]	Aluminum module area
$S_{Al,av,row}$	[m2]	Aluminum area of fan-shape row

P_d	[MPa]	Design pressure
σa	[MPa]	Allowable stress
V_{Al}	[m3]	Total aluminum volume
θ	[degrees]	Central angle of module section
α	[degrees]	Central angle of module
Nu	[-]	Nusselt number
Re	[-]	Reynolds number
Pr	[-]	Prandtl number

NEW SOLAR THERMAL POWER PLANT CONCEPT

Figure 1 presents the new solar thermal power plant concept. Solar beams are reflected by many heliostats placed on the ground and are directed to the central mirror, where they are reflected again to the downward direction. They are collected at the receiver, which is placed on the tower type structure. To collect the beams effectively, a compound parabolic concentrator (CPC) is provided on the receiver. The receiver resembles a vertical cave with a small opening on the top. Within the cave, the sun beams repeat absorption and reflection. A major fraction of the energy is transferred to the aluminum blanket while the residual small energy is dissipated by heat transfer and heat radiation from the top opening.

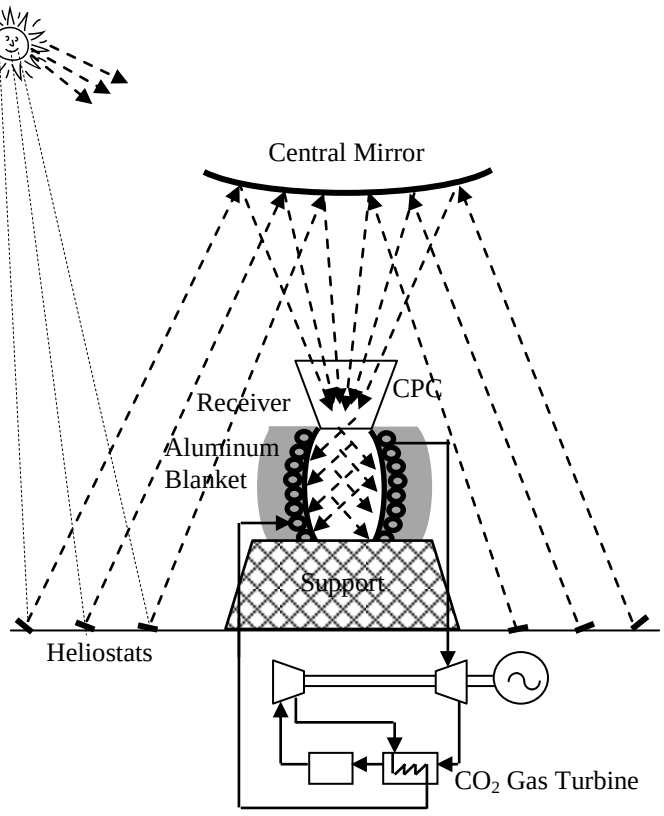

Figure 1 New concept of solar thermal power plant

SOLAR ENERGY RECEIVING EFFICIENCY

Some fraction of the thermal energy collected by the receiver is dissipated to the outside by heat transfer and heat radiation, thereby becoming heat loss. As the temperature of the working fluid increases, the receiver surface temperature increases and the heat loss increases. Then, the receiver efficiency $\eta_{receiver}$ decreases. Among the heat losses, effects of the radiation heat loss are considerably large because it is proportional to the fourth power of the absolute temperature of the heat transfer surface. The total thermal efficiency η is defined by the following equation.

$$\eta_{total} = \eta_{receiver} \times \eta_{cycle} \quad (1)$$

Then, even if the cycle thermal efficiency η_{cycle} increases with the temperature increase, η_{total} decreases because of the reduction of $\eta_{receiver}$.

To solve this problem, a beam down solar beam collection system is effective. In this system, the solar beams are collected at the central mirror and are reflected downward and emitted into the receiver cave. The radiation beams repeat reflections within the cave. The beam dissipation is possible only from the small upper opening. Therefore, large amounts of energy are absorbed by the receiver wall. The heat loss is small.

Figure 2 shows the receiver efficiency for both the tower top and the beam down systems. In these calculations, the working fluid flows in the ring annulus space on the receiver surface. Calculations were conducted for the molten salt or the supercritical CO_2 gas. For molten salt, a temperature difference of 20 K was assumed between the molten salt and the turbine working fluid. The receiver efficiency is known to be higher for the beam down system than for the tower top system, which is magnified with the temperature increase.

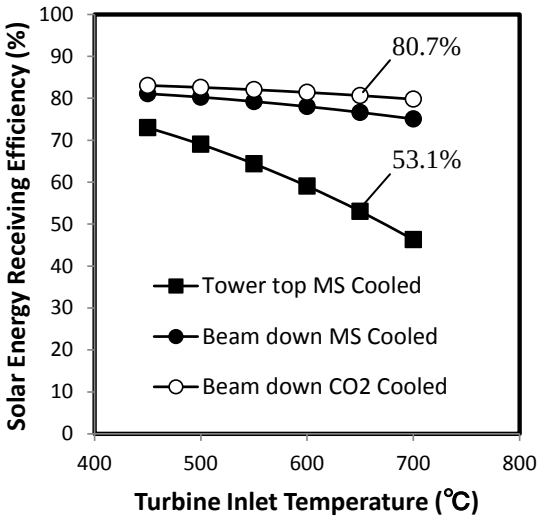

Figure 2 Solar energy receiving efficiency for the tower top and the beam-down systems

RECEIVER STRUCTURE AND HEAT STORAGE BY ALUMINUM

Validation of Numerical Models

Reportedly, molten salt (a mixture of 60% $NaNO_3$ and 40% KNO_3) cannot be used at temperatures higher than 600°C. For that reason, this fluid is unsuitable for a gas turbine cycle. Therefore, aluminum is used instead. Aluminum is useful at higher temperatures and is a good heat transfer material, with

extremely high thermal conductivity (237 W/m/K). Moreover, it is useful as a phase change heat storage material. It melts at 660°C, and its heat of fusion is extremely large (397 kJ/kg). Its specific heat is also high (0.9 kJ/kg/K). The aluminum is charged in a ring shape vessel of the receiver wall. Numerous heat transfer tubes of turbine working fluid are provided within the aluminum. The ring shape vessel is divided into many triangular modules, as shown in Figure 3. Solar beams are introduced into the gaps between the triangular modules and reach the depth. This structure is effective to achieve a large receiver heat transfer surface and to reduce the surface temperature.

When the receiver receives solar energy in the morning, the heat energy is used to raise the aluminum temperature. Then it is transferred to the fluid (CO_2). The aluminum temperature increases gradually and reaches 660°C at the area of the CO_2 outlet. The solar energy is used to melt the aluminum, storing the latent heat. In the evening, the solar energy decreases gradually. The supplied heat becomes less than the heat transferred to the fluid. The aluminum temperature then begins to decrease. The molten aluminum again begins to solidify. During solidification, the heat to raise the turbine fluid is supplied by the heat of fusion of the aluminum. However, in the fluid inlet area, the aluminum temperature is always less than 660°C. After all the aluminum has solidified, the heat needed during the night is supplied by the sensible heat because of the temperature reduction.

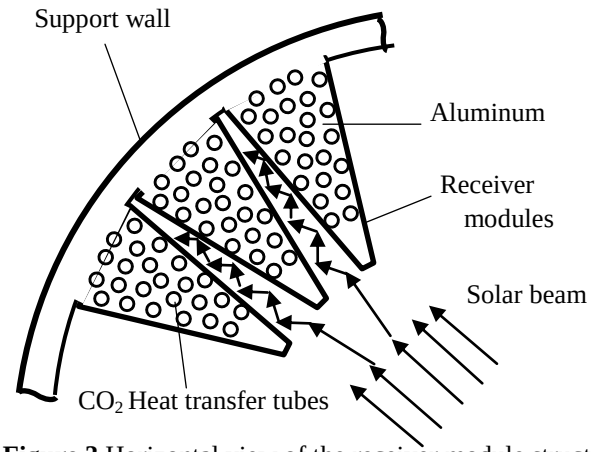

Figure 3 Horizontal view of the receiver module structure

A vertical view of the receiver is presented in Figure 4. Solar beams are collected to the receiver cave using the compound parabolic concentrator (CPC). Except for the receiver outer diameter, all dimensions were determined based on an earlier report in the literature [4]. These dimensions correspond to a 100 MWt class plant, where the outer diameter of the heliostat field is 800 m. Actually, 122 MW solar beams are emitted at the bottom of CPC. Because about 20 MWt energy is dissipated by heat transfer and heat radiation to the outside from the CPC top, roughly 100 MWt energy enters the receiver. The 28 m outer diameter was determined to ensure the requested aluminum inventory for the heat storage.

Because the diameter of the receiver cave opening is 9.2 m, the opening has an area of 66.5 m^2, which is much smaller than the tower top type receiver outer surface area. Therefore, the beam down receiver is markedly more effective than the tower top type to reduce the amount of heat loss. This benefit becomes great for high temperatures because the radiation heat is proportional to the fourth power of the surface temperature.

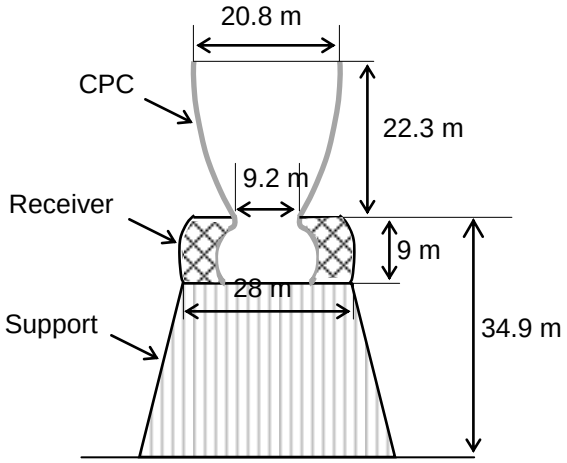

Figure 4 Vertical view of the receiver

SIMPLIFIED HEAT TRANSFER ANALYSES AND RECEIVER MODULE DIMENSIONS

Simplified Analyses

Simplified heat transfer analyses have been conducted under the following assumptions.

Net solar energy input to the receiver	100 MWt
CO_2 outlet pressure	20 MPa
CO_2 outlet temperature	650°C
CO_2 inlet temperature	467.63°C
Receiver vessel inner diameter D_1	16 m
Receiver vessel outer diameter D_2	28 m
Receiver vessel height	9 m
Receiver vessel upper opening diameter	9.2 m
Receiver module vessel wall thickness	20 mm
Heat transfer tube outer diameter	34 mm
Heat transfer tube inner diameter	24 mm

The CO_2 outlet pressure and the CO_2 inlet temperature are optimal values for the 650°C supercritical CO_2 gas turbine. The 304SS receiver wall thickness was chosen to bear the pressure caused by the weight of the stored aluminum. The tube wall thickness was ascertained as follows.

$$\text{Wall thickness tmin} = \frac{Pd \times Dout}{2 \times (\sigma a + Pd)} \qquad (2)$$

$\text{Pd} = 20\text{MPa} \times 1.2 = 24\text{MPa}$

$\text{Dout} = 34\text{mm}$

$\sigma\,\text{a} = \text{Allowable stress at 700°C for 304SS} = 27.5\text{MPa}$

$\text{Minimum wall thickness, tmin} = 7.92\text{mm}$

Therefore, 8 mm wall thickness was chosen.

A horizontal view of the module is shown in Figure 5.

Module radial length L_m is given for the center angle θ.

$$Lm = \sqrt{\frac{D_1^2}{4} - \frac{D_1 \times D_2}{2} cos\left(\frac{\theta}{2}\right) + \frac{D_2^2}{4}} \quad (3)$$

In the radial direction, the tube arrangement forms rows. Heat transfer tubes are arranged circumferentially for each row. In one row, at least two tubes are provided. There is no tube in the tip section, of which the outer surface is coated with a material of the minimum emission coefficient to reflect all beams to the greatest degree possible. An effective area within a module neglecting the tip section is denoted as $S_{eff,m}$. The radial length, except for the tip section, forms an effective length L_{eff}. The maximum row number becomes the following.

$$Nrow = \frac{Effective\ length\ Leff}{Pitch} \quad (4)$$

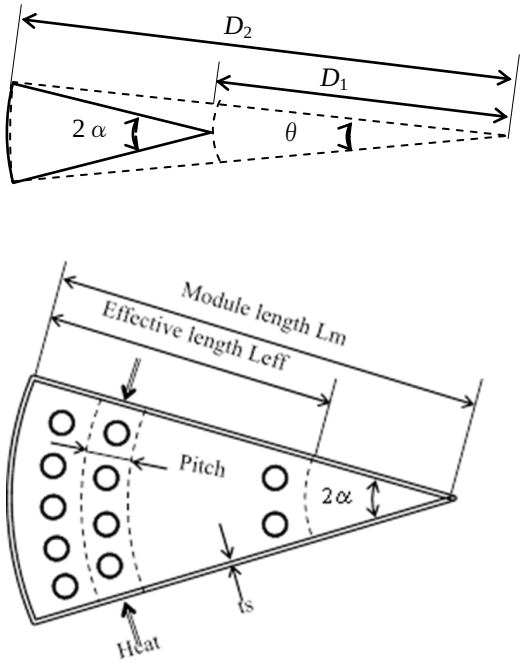

Figure 5 Sectional view of a module

Heat transfer tubes are arranged almost triangularly. Then, a unit area S_{unit} allotted for one tube is given as shown below.

$$Sunit = Pitch \times \frac{\sqrt{3}}{2} Pitch \quad (5)$$

Within a module, the possible number of tubes is the following.

$$Ntube, m = \frac{Seff, m}{Sunit} \quad (6)$$

The aluminum area of a module is calculated as shown below.

$$SAl, m = Seff, m - \frac{\pi}{4} Dout^2 \times Ntube, m \quad (7)$$

The total aluminum volume is given as presented below.

$$VAl = SAl, m \times Nm \times H_R \quad (8)$$

As described in this paper, the average temperature characteristics are calculated using a simplified method. First, a row with an average number of tubes is regarded as shown in Figure 6. A tube number in the row is given as follows.

$$Ntube, av, row = \frac{Ntube, m}{Nrow} \quad (9)$$

An aluminum area within a row is given.

$$SAl, av, row = \frac{SAl, m}{Nrow} \quad (10)$$

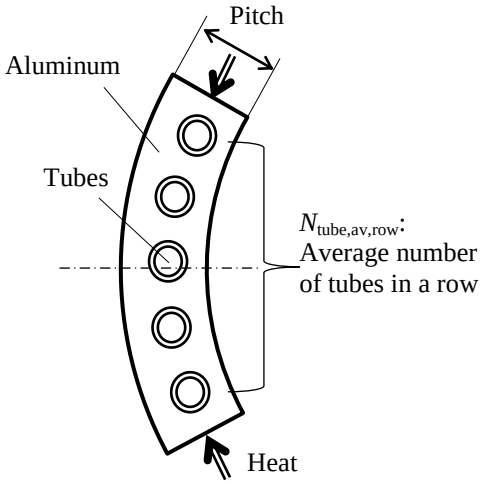

Figure 6 Row model provided with an average number of tubes

The heat transfer model is simplified further. Heat transfer in a half area of the fan-shaped row above is assumed to be equivalent to that in the trapezoidal area, as shown in Figure 7, where the total outer surfaces of the tubes of $N_{tube,av,row}$ is substituted by a straight surface with equal area.

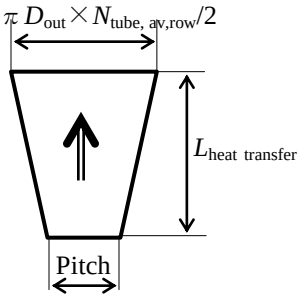

Figure 7 Trapezoidal heat transfer model

An equivalent heat transfer length L_{heat} transfer is assumed to be represented by dividing the thermal conduction area by the high temperature side boundary length, as shown in the following equation. Therein, half of the row area is considered.

$$\text{Lheat transfer} = \frac{SAl, av, row}{2 \times Pitch} \quad (11)$$

Using the simplifications above, two-dimensional analyses are converted to one-dimensional analyses. Although the actual structure is three-dimensional, the radial length is sufficiently short compared to the height. Vertical heat conduction will be extremely small and be regarded as negligible. Therefore, one-dimensional analyses are justified.

The following well-known equation was used for the heat transfer of CO_2 gas flow.

$$\text{Nu} = 0.023 Re^{0.8} Pr^{0.4} \quad (12)$$

Physical properties of CO_2 are based on the PROPATH dataset [5]. The phase change was not considered. The value of thermal conductivity of solid aluminum was used.

Determination of Dimensions

For the parameters of a receiver vessel outer diameter D_2, a module central angle θ and a tube pitch, heat transfer calculations were conducted. The aluminum volume, the heat storage amount, the maximum aluminum temperature, and the maximum vessel wall temperature were examined. Therein, the aluminum area exceeding 660°C was judged to have been melted.

Vessel diameter D_2 was varied: 24 m, 28 m, and 32 m. As D_2 becomes larger, both the vessel wall and aluminum temperatures decrease. Heat storage increases. The larger D_2 denotes a higher capital cost. D_2=28 m was selected as an appropriate value from economic aspects.

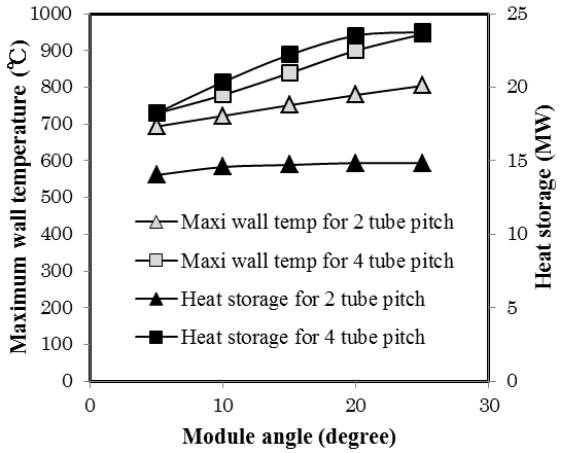

Figure 8 Module angle and tube pitch effects on the maximum wall temperature and the heat storage

Figure 8 presents effects of the module central angle θ and the tube pitch on the maximum wall temperature and the heat storage amount. The heat storage amount for the tube pitch of twice the diameters is too small, irrespective of the module angle because the aluminum area is limited. Then, 3-tube pitch or 4-tube pitch is appropriate. As described in this paper, the 4-tube pitch was selected.

The larger module angle necessitates the larger heat transfer length, which leads to a higher wall temperature. A module angle of 5 deg. was selected to achieve the lowest wall temperature.

Temperature Distribution in Aluminum

The temperature distribution is shown in Figure 9. Although the uniform thermal flux of solar beams is assumed, the axial temperatures differ because the CO_2 temperature at the inlet is 467.63°C. That at the outlet is 650°C. The maximum temperature becomes 695°C at the outlet in the near wall mesh. The lowest temperature occurs at the inlet in the vessel side mesh and 513°C. Only aluminum of 15 meshes melted among 100 meshes. Therefore, the melted zone was only 15%. However, a considerable amount of thermal energy is obtainable using the sensible heat under the assumption that heat capacity during temperature reduction of 100°C is available.

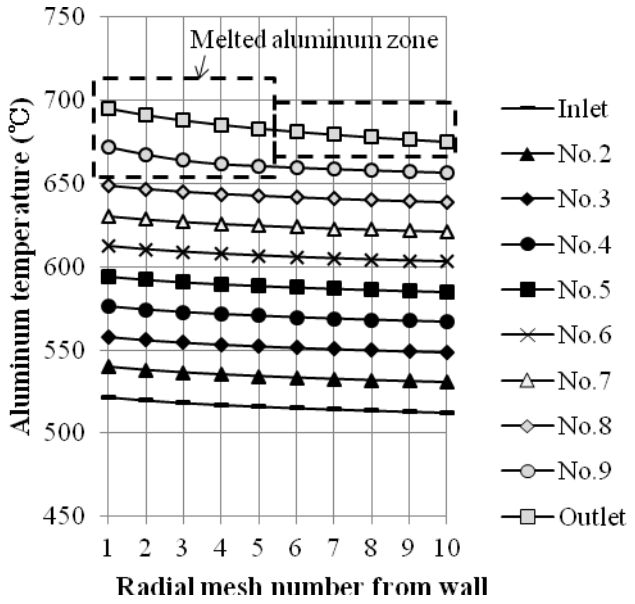

Figure 9 Temperature distribution of aluminum

POWER GENERATION BY SUPERCRITICAL CO_2 GAS TURBINE

Cycle thermal efficiencies were calculated for one intercooled supercritical CO_2 closed cycle under the following assumptions.

Turbine inlet pressure	20 MPa
Turbine inlet temperature	650°C
Compressor inlet temperature	35°C
Recuperator average temperature effectiveness	91%
Turbine adiabatic efficiency	92%
Compressor adiabatic efficiency	88%
Pressure drop for components (including piping)	

Receiver	2%
Recuperator high-temperature side	1.2%
Recuperator low-temperature side	0.4%
Precooler	1.0%
Intercooler	0.8%
Generator efficiency	98.5%

Figure 10 shows the heat balance for the turbine pressure ratio of 2.88 and the low-pressure compressor pressure ratio of 1.24. Maximum cycle thermal efficiency of 48.91% was achieved. The power generation efficiency was 48.18%.

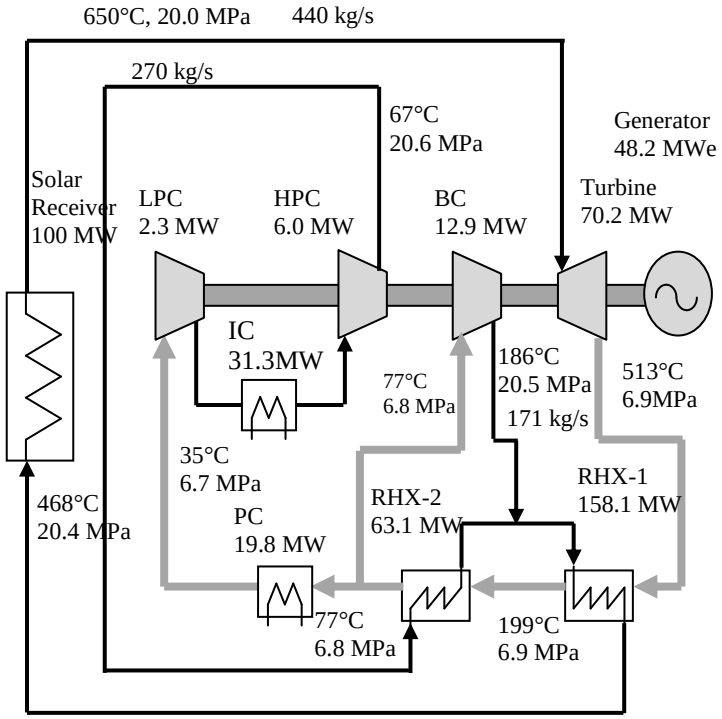

Figure 10 Flow diagram and heat balance for the supercritical CO_2 gas turbine.

In summary, for solar energy reflected by the central mirror, net energy of 100 MW is supplied to the receiver. Because the energy stored in aluminum using both the latent heat and the sensible heat is 725,000 MJ, the available thermal energy becomes 16.8 MWt for 12 hr. Therefore, the available power quantities during daytime (8:00–20:00) and at night (20:00–8:00) respectively become 83.2 MWt and 16.8 MWt. For electric power, it becomes 40.1 MWe and 8.1 MWe for the daytime and night, respectively, although the power at night is somewhat less because of the somewhat lower cycle thermal efficiency. These energy flows are presented in Figure 11.

CONCLUSION

A new solar thermal power plant is introduced, consisting of a beam down solar receiver, an aluminum heat transfer and heat storage system, and a supercritical CO_2 gas turbine. The beam down receiver has higher receiver efficiency of 80.7% than the tower receiver of 53.1% at the turbine inlet temperature of 650°C. Triangular aluminum modules are effective to achieve a large heat transfer area to reduce the wall surface temperature. As results of simplified one-dimensional heat transfer analyses, optimal dimensions were ascertained for a receiver vessel diameter, a module central angle and a tube pitch. For these dimensions, the aluminum melting area became 15%. Quantities of available heat stored using latent heat and sensible heat are, respectively, 216,000 MJ and 509,000 MJ. The total heat became 725,000 MJ. The power generation efficiency is 48.18% at 650°C turbine inlet temperature for the supercritical CO_2 gas turbine. The available daytime power and night power respectively become 40.1 MWe and 8.1 MWe.

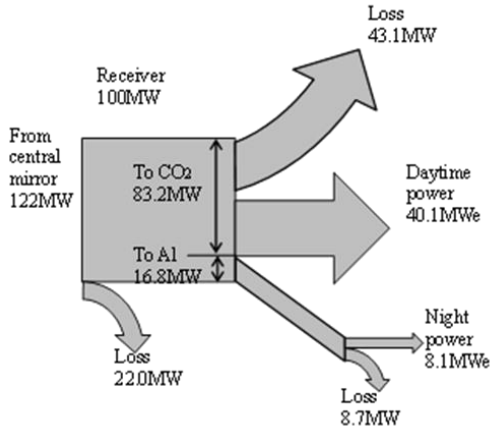

Figure 11 Energy flow for a solar thermal power plant

REFERENCES

[1] Kato Y., Nitawaki T., and Muto Y., Medium temperature carbon dioxide gas turbine reactor, *Nuclear Engineering and Design*, Vol. 230, 2004, pp. 195-207

[2] Muto Y., and Kato, Y., Cycle thermal efficiency of supercritical CO_2 gas turbine dependent on recuperator performance, *Journal of Power and Energy Systems*, Vol. 7, No. 3, 2013, pp. 1-14

[3] Muto Y., Aritomi M., Ishizuka T., and Watanabe N., Comparison of supercritical CO_2 gas turbine cycle and Brayton CO_2 gas turbine cycle for solar thermal power plants, *The Fourth International Symposium – Supercritical CO_2 Power Cycles*, September 9-10, 2014, Pittsburgh, Pennsylvania

[4] Hasuike H., Yosizawa Y., Suzuki A., and Tamaura Y., Study on design of molten salt solar receivers for beam-down solar concentrator, *Solar Energy*, Vol. 80, 2006, pp. 1255-1262

[5] PROPATH group, 1990, PROPATH: *A Program Package for Thermo-physical Properties of Fluids, Version 10.2*, Corona Publishing Co., Tokyo, Japan, 1990.

ACKNOWLEDGMENTS

The authors are grateful to Chairman F. Urano and Vice-chairman H. Mimura of Smart Energy Solutions Association (SESA) for their cooperation in research related to development of the supercritical CO_2 gas turbine and solar thermal power plant.